CIGRÉ-787 **2016 CIGRÉ Canada Conference**
21, rue d'Artois, F-75008 PARIS
http : //www.cigre.org Vancouver, BC Canada, October 17-19, 2016

Transient Stability Assessment of BC Hydro Power System Using Decision Trees

Matin Rahmatian[1], Yu Christine Chen[1], William Dunford[1], Ali Moshref[2]
The University of British Columbia[1], BBA Power Corporation[2]
Canada

SUMMARY

Transient stability assessment (TSA) is an important issue for BC Hydro's power system. Supervisory control and data acquisition (SCADA) systems commonly operating in power system control centres cannot support all critical TSA functions in real time. Emerging synchrophasor-based wide-area monitoring systems (WAMSs) enable real-time monitoring of power systems. Synchrophasors measured by phasor measurement units (PMUs) at a rate of 60 samples per second (or faster) along with fast communication infrastructure make it possible to perform TSA in real time.

In this paper, the capabilities of WAMSs for TSA are demonstrated and compared with SCADA-based systems using automatic learning techniques, specifically via decision trees (DTs). The focus of the study is on the Northern Intertie, which connects BC Hydro (BCH) and Bonneville Power Administration (BPA) systems. The Western Electricity Coordinating Council (WECC) operation planning models are used to generate a synthetic data set, which includes 200 system snapshots corresponding to the summer of 2013, and covers different operating conditions for the Northern Intertie. The Northern Intertie transfers up to 2200 MW between BCH and BPA systems. The BCH system is also connected to Alberta Electric System (AES) on the east. These systems are interconnected via two interties enabling BCH and AES to transfer up to 800 MW.

Credible *N-k* (*k* = 1, 2, 3, and 4) contingencies are selected to provide the study with enough unstable cases in the data set. The faults mostly occur in 500-kV backbone of the system while transferring large amounts of power between the BCH and BPA systems. Circuit breakers are assumed to operate after 3 cycles. In total, 9474 different time-domain simulation cases are obtained using the TSAT software, out of which 1088 cases are unstable and the remaining are stable.

We assume that PMUs are installed at major power plants in the BCH, AES and BPA systems, interties with BCH's neighbouring systems, as well as critical corridors transferring power from northern BC to the lower mainland. Accordingly, different real-time synchronized measurements and indices obtained from the WAMS in pre- and post-contingency operating conditions are used as feature sets.

To highlight the difference between SCADA system and WAMS capabilities for real-time TSA, we use various features to train DTs. The SCADA system is characterized by low sampling rates and data transfer speeds as well as unavailability of real-time phase-angle measurements. Thus, to emulate the SCADA system, DTs are first trained and tested using the relative angle and active-power values obtained from the pre-fault operating condition. In the case of using WAMS, on the other hand, we assume the availability of post-fault features, such as bus-voltage phase-angle differences across the

system, as well as features obtained based on centre of inertia (COI) and energy functions. The DTs obtained using SCADA and WAMS measurements are tested against new unseen cases, and prediction accuracy rates are compared between the two monitoring systems. In this paper, we demonstrate that a reliable real-time TSA tool can be built using WAMS measurements, which is superior to using only SCADA measurements.

KEYWORDS

Transient Stability Assessment, Supervisory Control and Data Acquisition, Wide-area Monitoring Systems, Automatic Learning.

1. INTRODUCTION

Most existing energy management systems use a SCADA system to monitor power systems. A SCADA system is typically composed of data acquisition and switching, communication system, and supervisory control. The data acquisition is performed using a remote terminal unit (RTU), which monitors parameters in the field and transmits data to the control centre. The RTU is capable of collecting measurements of voltage magnitudes, active- and reactive-power injections, and equipment status. The data is scanned and sent to the control centre by the supervisory control system in a period of several seconds [1]. However, the SCADA system cannot be used to monitor a power system in real time or even near real time. This is because of the slow communication of unsynchronized data to the control centre. To enable a real-time monitoring system, it is necessary to send the time-synchronized data to the control centre several times in a second. Moreover, for many functions, such as TSA, it is necessary to have voltage and current data. To this end, a synchrophasor-based WAMS enables fast real-time monitoring of power systems. Here, synchrophasors measured by PMUs at various buses at a rate of 60 samples per second (or faster) together with fast communication infrastructure make possible many online monitoring and control applications, such as real-time TSA [2].

Real-time TSA is an important task in modern electric power systems, since they face new problems such as increased electricity demand, large blackouts, and uncertainties from renewable energy resources. These circumstances reveal the need for better tools to monitor transient stability [3]. There are three main strategies for TSA: time-domain (T-D) approaches, direct approaches, and automatic learning (AL) approaches [4]. Of these, T-D approaches require data related to the system model, operating condition, and the occurring disturbance. Processing all this data leads to a heavy computational burden , so parallel computation methods are proposed in the literature [5]. In direct approaches, an energy function is defined to estimate the amount of critical energy that can be absorbed by the system before fault clearance. Such energy functions are difficult to obtain for large-scale power systems [6]. On the other hand, AL approaches have been tested on actual large-scale power systems in the past [7]-[9]. For example, a comprehensive database of the Hydro-Québec power system is constructed in [10]. Wide-area severity indices obtained based on voltage criteria in time-domain are applied while a DT is used as the classifier. A random forest (RF) classifier is used in [11]. In [12], it is shown that RFs can operate efficiently in the presence of small changes in the network topology and different dynamics of the power system. In [13], both static and dynamic security are considered. Here, regression trees have been applied to indicate the number of overloaded lines and voltage magnitude violations following a contingency.

In this paper, we implement and compare a classification tool to assess transient stability that synthetic data to simulate a traditional SCADA system and a new hypothesized synchrophasor-based WAMS installed in the actual BCH power system. The classification tool used in our study is classification and regression tree (CART), which is a well-known algorithm for developing DTs [14].

2. WIDE-AREA SECURITY INDICES

With regard to TSA, numerous features or indices have been proposed to be applied to classifiers. For a WAMS, a vast variety of features can be applied including pure real-time measurements obtained from the power system and more complicated indices or features resulting from computations involving such measurements [10]-[13]. However, based on the SCADA system characteristics, the only features that can be applied are pre-fault angles and active powers. In this section, we describe

TSA indices used in our work, which can be categorized as (i) pure measurement indices, (ii) COI-referred indices, and (iii) energy function-based indices.

A. Pure Measurement Indices

Pure measurement indices can be obtained from a SCADA system. However, these measurements are not synchronized, nor are they obtained in real time. Therefore, they are just related to the pre-fault conditions. On the other hand, we select several synchronized measurements from the pre- and post-fault systems and use them as TSA indices. With regard to pre-fault measurements, we use the total active-power generation of major power plants in each region, the active-power generation of each individual major power plant, the voltage phase angles of buses connected to major power plants and those of interface buses, the active-power flow across interties connecting the regions, and the active-power flow across critical long transmission lines. Under post-fault conditions, we use time-synchronized measurements of voltage phase angles at the buses connected to major power plants and at buses that interface between two regions. These indices can only realistically be measured by the WAMS.

B. COI-Referred Indices

Since deviation from the COI angle can indicate system stress, below, we introduce COI-referred response signals. These indices should be obtained in real-time ; therefore, they can only be obtained from a WAMS and not a SCADA system. Consider an interconnected power system in which the monitored region k has K-1 neighbouring regions. Assume we monitor region k and it contains N_k major synchronous generators to be monitored. Denote, by $P_{mi}(t)$ and $P_{ei}(t)$, the mechanical power input [p.u.] and the electrical power output [p.u.], respectively, of generator i at time t. Let $\delta_i(t)$ and $\omega_i(t)$ denote the rotor angle [rad] and speed [rad/s], respectively, of generator i at time t; and let M_i denote the inertia constant [s^2/rad] of generator i. With these notations in place, we next describe COI-referred indices that are applied to our TSA algorithm. First, we compare the pre- and post-fault conditions and propose the following centre deviation index:

$$\Delta\delta_k(t) = \frac{\delta_{COI,k}(t) - \delta_{COI,k}^{pre-fault}}{\delta_{COI,k}^{pre-fault}}, \tag{1}$$

where $\delta_{COI,k}(t)$ denotes the COI angle of region k at time t, and $\delta_{COI,k}^{pre-fault}$ represents the pre-fault COI angle of region k. Next, we also apply [15]

$$\alpha_k(t) = \sum_{i=1}^{N_k} f_i(t)\left(\omega_i(t) - \omega_{COI,k}(t)\right), \tag{2}$$

where $f_i(t) = P_{mi}(t) - P_{ei}(t) - \frac{M_i}{\sum_{i=1}^{N_k} M_i} P_{COI,k}(t)$, with $P_{COI,k}(t) = \sum_{i=1}^{N_k}(P_{mi}(t) - P_{ei}(t))$,

$$\beta_k(t) = \sum_{i=1}^{N_k} f_i(t)\left(\delta_i(t) - \delta_{COI,k}(t)\right), \tag{3}$$

and,

$$\gamma_k(t) = \sum_{i=1}^{N_k}\left(\omega_i(t) - \omega_{COI,k}(t)\right)\left(\left(\delta_i(t) - \delta_{COI,k}(t)\right) - \left(\delta_i^{pre-fault} - \delta_{COI,k}^{pre-fault}\right)\right), \tag{4}$$

where $\delta_i^{pre-fault}$ denotes the pre-fault angle of generation i. In addition to the indices described in (1)–(4), we modify $\gamma_k(t)$ in (4) to reflect the behaviour of the COI angle and speed, and include the following index:

$$\sigma_k(t) = \omega_{COI,k}\left(\delta_{COI,k}(t) - \delta_{COI,k}^{pre-fault}\right). \tag{5}$$

Moreover, aimed at an index that is sensitive to loss of synchronism, we make use of the integral square generator angle (ISGA) index, which is expressed as [16]

$$J = \frac{1}{T}\int_0^T \frac{1}{M_{total}} \sum_{i=1}^{N_k} M_i\left(\delta_i(t) - \delta_{COI,k}(t)\right)^2 dt, \tag{6}$$

where T represents the observation time window.

For TSA, it is not only important to consider characteristics of the monitored region, but to also account for interactions between the monitored region and its neighbours. To this end, we consider the centre of angle stability index, expressed as [17]

$$\Delta\delta_{k,j}(t)=\left|\frac{\delta_{COI,k}(t)-\delta_{COI,j}(t)}{\delta_{COI,k}^{pre-fault}+\delta_{COI,j}^{pre-fault}}\right|\times 100\,, \tag{7}$$

which can be interpreted as the angle deviation between regions *k* and *j*. Finally, to assess the coherency between a region and its neighbouring regions following a fault, we consider COI angle and rotor speed of region *k* and *j* as a criterion and calculate the rms-coherency between them, as [18]

$$\psi_{k,j}=\left[\frac{1}{T}\int_0^T\left((\delta_{COI,k}(t)-\delta_{COI,j}(t))^2+(\omega_{COI,k}(t)-\omega_{COI,j}(t))^2\right)dt\right]^{1/2}, \tag{8}$$

where *T* represents the observation time window. To summarize, we consider COI-referred indices (1)–(8) in our TSA algorithms.

C. Energy Function-Based Indices

Assuming the remainder of the system can be modelled as an infinite bus, let $V_i(t)$ and $U_i(i)$ denote the kinetic energy and potential energy functions of generator *i*, respectively.
Similar to the COI-referred, the indices proposed here can only be obtained using a WAMS. As an indicator of transient stability in region *k*, we propose to apply the following total potential energy index:

$$U_{total,k}(t)=\sum_{i=1}^{N_k}U_i(t)\,, \tag{9}$$

and the following total kinetic energy in region *k*

$$V_{total,k}(t)=\sum_{i=1}^{N_k}V_i(t)\,. \tag{10}$$

A kinetic energy separation index, formulated as

$$\Delta V_{k,j}(t)=\left|\sum_{i=1}^{N_k}V_i(t)-\sum_{i=1}^{N_j}V_i(t)\right|, \tag{11}$$

is used in our proposed TSA algorithms. In summary, we consider energy-based features in (9)–(11) in training CART models for real-time TSA.

3. Simulation results

In this section, details of the power system models used in the paper and simulation methods are described. Next, DTs are developed using CART [14] based on the SCADA system and the synchrophasor-based WAMS. The TSA capabilities of the DTs trained with SCADA and WAMS measurements are discussed and compared. According to the standards of North American Synchrophasor Initiative (NASPI), PMUs should be installed at major power plants with high generation capacity and critical corridors. In the present study, it is assumed that all major power plants with high generation capacity in the three power systems (5 in BCH, 7 in AES, and 12 in BPA), the interties between the three systems, and also a major corridor transferring power from the major power plants located in the northern part of BCH are equipped with PMUs. Consequently, power flows, angles, voltage magnitudes and frequencies at these substations are accessible at the control centres through the WAMS. For the SCADA system, we consider the same measurement locations. However, there are some limitations such as communications speed and synchrophasor measurements. Therefore, we assume that only the pre-fault active-power values and the pre-fault calculated relative angles are accessible at the control centre, not in real time nor synchronized.

A. Power system model

For the simulations, 200 power flow base cases of the WECC power system of the summer 2013, covering different operating conditions of the Northern Intertie are selected. In these cases, the active-power exchange is varied between 3700 MW from North to South and 2450 MW South to North. We

extend the active-power exchange beyond the operational limits to induce unstable cases. Here, some operationally valid N - k (k = 1, 2, 3, and 4) contingencies are selected to provide the study with enough unstable cases in the data set. The contingencies mostly occur in the 500 kV backbone of the system, transferring large amounts of active power between the BCH and BPA systems. In total, 48 contingencies are selected. To cover a wider range of operating conditions, three different topologies of the power system around the Northern Intertie are considered. Therefore, 9474 different time-domain simulation cases are obtained using TSAT software, out of which 1088 cases are unstable and the remaining stable [19]. Based on the operational standards of BCH, every fault in the 500 kV of the system should be cleared after three cycles [20]. Therefore, in all of the simulations, the fault occurs at the time instant of 100 ms and lasts for 3 cycles, i.e., 50 ms.

B. Time-domain simulations

Figure 1 shows an unstable simulation case. Note that the rotor angles diverge and divide into three groups after fault clearance. Each of these three groups belongs to one of the power systems under the study, i.e., BPA, BCH and AES. From this, we infer that the coherent regions have been considered correctly in our study. The simulation results for some of the wide-area transient stability indices are shown in Fig. 2. Here, three different power flow cases are selected, and different contingencies are selected that lead to both stable and unstable cases. In Fig. 2, the proposed wide-area transient stability indices based on the COI are plotted for BCH for during-fault and post-fault periods. These features are indeed capable of discriminating between stable and unstable cases.

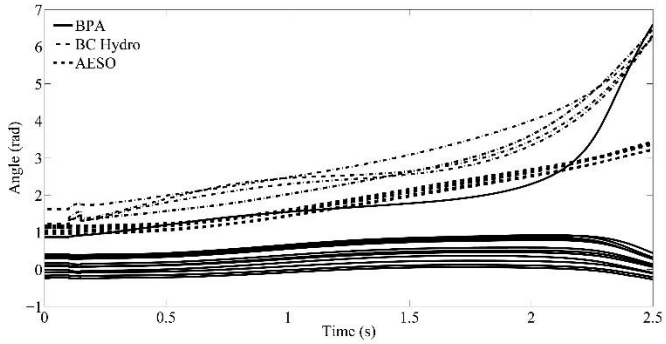

Fig. 1. A transiently unstable case following a fault occurrence.

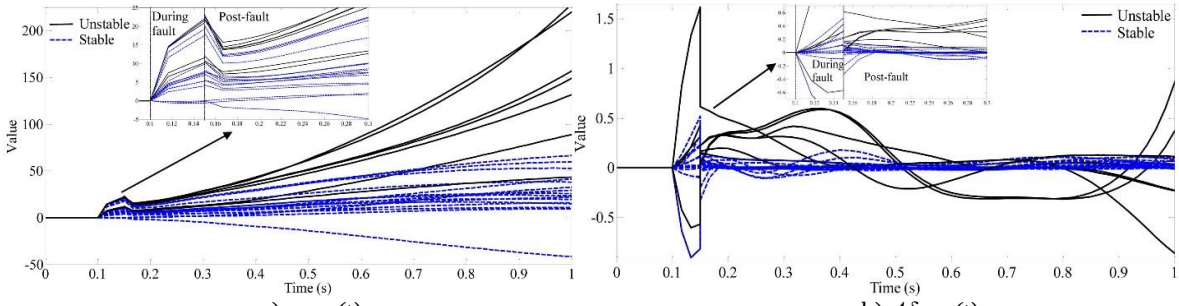

a) $\alpha_{BCH}(t)$ b) $\Delta\delta_{BCH}(t)$

Fig. 2. Characteristic of two COI-referred indices following different faults in three different power flow patterns.

C. Classification results

First, we use only the pre-fault features which are available from the SCADA system, to train a CART model. These features include pre-fault active-power generation of the main power plants in BCH, BPA and AES, interchanging active power between the regions, active-power transfer from the northern part of BC to the lower mainland and also, the pre-fault angles. The resulting DT is depicted in Fig. 3. By testing this DT with unseen cases, we find that the prediction accuracy of the developed model is 55.41%, which is not satisfactory. However, it can be observed that the more important pre-fault features are power generation of BCH system, active-power transfer between BCH and BPA and active-power transfer from the northern BC to the lower mainland. The obtained features and the thresholds can be used as a guide on transient stability limits for the system operators.

Next, we train a CART model with both the pre- and post-fault features which are available in the WAMS. In addition to the pre-fault features, we use post-fault features in the first five cycles after fault clearance, which is feasible according to the characteristics of synchrophasor-based WAMS [19]. The obtained model for the 4th cycle after fault clearance is depicted in Fig. 4. Here, the prediction accuracy rates increase to around 99% and most of the selected features are post-fault features. It can be observed that α_{BCH} has been selected as the root node in the obtained DT, and generally, the synthesized features selected in all the obtained DTs are COI- or energy function-based which shows their ability to distinguish stable and unstable cases in comparison to pure relative angle features. For the interested reader, more results and further discussions can be found in [19].

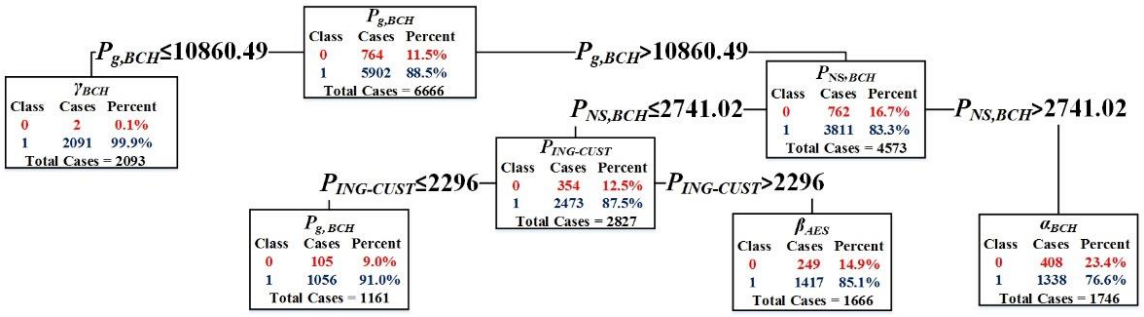

Fig. 3. CART model obtained using SCADA system measurements

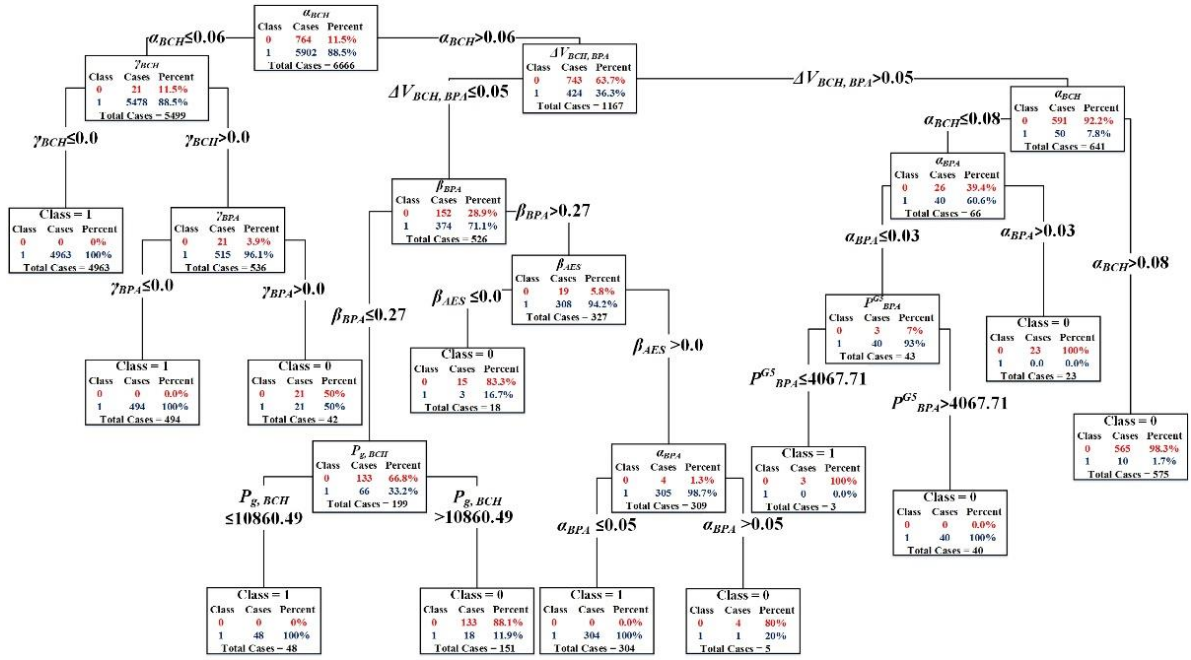

Fig. 4. CART model obtained using the WAMS measurements

4. Concluding Remarks

Synchrophasor-based WAMSs provide more capabilities for real-time monitoring of the modern power system in comparison to SCADA systems. Real-time TSA is more effective with a WAMS as compared with the conventional SCADA-based system. In this paper, the automatic learning approach is used to compare the applicability of SCADA systems and WAMSs for real-time TSA in the actual power system model of BC Hydro. First a consistent data sat is built using different power flow base cases in three topologies and credible contingencies. Next, different features or indices are calculated for each simulation case, using which DT models are trained. The results show higher prediction accuracy rates of DTs trained with features obtained from the WAMS.

REFERENCES

[1] E. Vaahedi, “Practical power system operation” (John Wiley & Sons 2014).
[2] D. Novosel, V. Madani, B. Bhargava, K. Vu, and J. Cole “Dawn of the grid synchronization” (IEEE Power and Energy Magazine, vol. 1, no. 6, pp. 49–60, 2008).
[3] Y. C. Chen and A. D. Domínguez-García “A method to study the effect of renewable resource variability on power system dynamics” (IEEE Transactions on Power Systems, vol. 27, no. 4, pp. 1978–1989, 2012).
[4] M. Pavella, D. Ernst, and D. Ruiz-Vega, “Transient stability of power systems: a unified approach to assessment and control” (Springer Science & Business Media, 2012).
[5] S. Zadkhast, J. Jatskevich, and E. Vaahedi “A multi-decomposition approach for accelerated time-domain simulation of transient stability problems” (IEEE Transactions on Power Systems, vol. 30, no. 5, pp. 2301–2311, 2015).
[6] A. Pai, Energy function analysis for power system stability. Springer Science & Business Media, 1989.
[7] R. Zhang, Y. Xu, Z. Y. Dong, and K. P. Wong “Post-disturbance transient stability assessment of power systems by a self-adaptive intelligent system,” (IET Generation, Transmission & Distribution, vol. 9, no. 3, pp. 296–305, 2015).
[8] A. Kaci, I. Kamwa, L. Dessaint, S. Guillon et al. “Synchrophasor data baselining and mining for online monitoring of dynamic security limits” (IEEE Transactions on Power Systems, vol. 29, no. 6, pp. 2681–2695, 2014).
[9] M. He, V. Vittal, and J. Zhang “Online dynamic security assessment with missing pmu measurements: A data mining approach” (IEEE Transactions on Power Systems, vol. 28, no. 2, pp. 1969–1977, 2013).
[10] I. Kamwa, S. Samantaray, and G. Joos “Development of rule-based classifiers for rapid stability assessment of wide-area post-disturbance records” (IEEE Transactions on Power Systems, vol. 24, no. 1, pp. 258–270, 2009).
[11] S. Samantaray, I. Kamwa, and G. Joos “Ensemble decision trees for phasor measurement unit-based wide-area security assessment in the operations time frame” (IET Generation, Transmission & Distribution, vol. 4, no. 12, pp. 1334–1348, 2010).
[12] I. Kamwa, S. Samantaray, and G. Joos “Catastrophe predictors from ensemble decision-tree learning of wide-area severity indices” (IEEE Transactions on Smart Grid, vol. 1, no. 2, pp. 144–158, 2010).
[13] R. Diao, V. Vittal, and N. Logic “Design of a real-time security assessment tool for situational awareness enhancement in modern power systems” (IEEE Transactions on Power Systems, vol. 25, no. 2, pp. 957–965, 2010).
[14] L. Breiman, J. Friedman, C. J. Stone, and R. Olshen, “Classification and Regression Trees” (Wadsworth, 1984).
[15] C. Fu and A. Bose “Contingency ranking based on severity indices in dynamic security analysis” (IEEE Transactions on Power Systems, vol. 14, no. 3, pp. 980–985, 1999).
[16] S. M. Rovnyak “Integral square generator angle index for stability assessment,” (in Proceedings of the IEEE Power Engineering Society Winter Meeting, 28 Jan–1 Feb., 2001).
[17] M. Rahmatian, W. G. Dunford, and A. Moshref “PMU based system protection scheme,” (in Proceeding of the 14th Electrical Power and Energy Conference (EPEC), 12–14 Nov., 2014).
[18] I. Kamwa, A. K. Pradhan, G. Joos, and S. Samantaray “Fuzzy partitioning of a real power system for dynamic vulnerability assessment” (IEEE Transactions on Power Systems, vol. 24, no. 3, pp. 1356–1365, 2009).
[19] M. Rahmatian, Y. C. Chen, A. Palizban, A. Moshref and W. G. Dunford, “Transient stability assessment via decision trees and multivariat adaptive regression splines,” (submitted to the journal of Electric Power System Research.)
[20] BC Hydro, Protection and Control Planning Department. “Bulk transmission circuit fault clearing time, internal report” (2015, April).